講演番号：082　文献番号：20185082

学術講演会予稿集正誤表
(Errata of Proceedings/Summarized Papers)

学術講演会セッション番号・セッション名 (SessionNo.-Session Name)	Session number 19 – Safety / Related Technology I
講演タイトル （Title）	Euro Ncap Far Side Sled Test And Tracking Methodology
講演者名 (Speaker name) 所属名 (Affiliation)	Genís Mensa – Applus IDIADA
誤 (Incorrect)	While doing the revision of the paper to prepare the presentation we have detected that this paper has many English errors that may lead to a vast amount of misunderstandings in the message that we (as a Department) wanted to convey.
正 (Correct)	This is a revised version of the same paper (instead of a simple errata) as the amount of changes to be done is considerably big. The only objective of this would be to try to improve the quality of the paper in order to have the best submission possible for the JSAE.

Euro Ncap Far Side Sled Test And Tracking Methodology

Genís Mensa [1)] Maria Odriozola [1)] Céline Adalian [1)] David Company [1)] Núria Parera [1)]

1) *Applus IDIADA, Passive Safety, L'Albornar PO BOX 20 E-43710, Santa Oliva (Tarragona), Spain (gmensa@idiada.com)*

ABSTRACT: Accident research supports the fact that there is a lack of occupant protection in far-side lateral crashes. Due to this, Euro NCAP is working on enhancing its protocols to focus on this area and promote vehicle improvements. The Euro NCAP roadmap for Far Side will be detailed in this paper, together with the current protocol, assessment method and an alternative methodology that has been developed by IDIADA to obtain extensive information of dummy head excursion by means of Tracking technology.

KEY WORDS: **Crash Test, Euro NCAP, Tracking, Methodology** Safety, Related Technology (A1)

1. INTRODUCTION

Global accident statistics show that side impacts are the second most common type of crash, after frontal impacts. For example, side impact crashes accounted for 25% of the total amount of fatal accidents that took place in 2016 in the US (1). This information has been retrieved from the Insurance Institute for Highway Safety (IIHS), which has one of the vastest databases, in relation to real-world severe crash tests in the US. A similar trend has been identified in Europe, where Side Impact road collisions correspond to approximately one quarter of the total amount of serious-to-fatal injuries (2).

Although vehicles have been improved in order to ensure occupant safety in side impact crash events, accident research data show that there is still a relatively high percentage of injuries and fatalities in this type of crashes. These injuries and fatalities can be found both when the impact is on the occupant's near side and its far-side. Table 1, shown below; shows four different accident scenarios that can be found when a side impact crash occurs, where the red dot represents the studied occupant.

Table 1 Side Impact Crash Configurations[(3)]

Legend	Far Side	Near Side
Alone	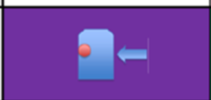	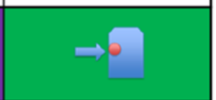
With close occupant		

Accident data from Germany and France showed real-world cases where belted front-row adult occupants sustained MAIS2+ (Moderate or above (4)) injuries. The results from the German Accident Reconstruction Database (GIDAS (5) showed that 26% (of the side impact crashes) had MAIS2+ injuries when the impact was on the passenger side with only the driver as a front occupant and 17% of the cases had MAIS2+ injuries when the impact was on the passenger side but both frontal passengers were in the vehicle. The results form the French database (LAB: Laboratory of Accident Analysis, Biomechanics and Human Behavior) showed that in 19% of the side impact crashes the occupant sustained MAIS2+ injuries when the impact was on the passenger side and there was only the driver sitting in the front row. On the other hand, when both front occupants were in the vehicle, the percentage of occupants that sustained MAIS2+ injuries was of 18%.(3) The accident study from which the previous data was extracted also also concluded that the proportion of occupants that sustained MAIS2+ injuries in Far Side load case scenarios with close occupant was not major than those Far Side cases in which te driver was travellin alone (in the first row).

2. FAR SIDE CRASH TEST

2.1. EURO NCAP SIDE IMPACT PROTOCOLS

Given the data shown above, the European New Car Assessment Programme (Euro NCAP) has decided to include a new test and assessment in their new protocol: The Far-Side Impact Assessment. According to the 2025 Road Map the test protocol for this new assessment was to be released in year 2018. The data from this test will be monitored for two years and it will be implemented in the official protocol in 2020 (6). Currently, the two side impact tests that are included in the Euro NCAP test protocol are the Oblique Side Pole Test (7) and the Side AE-MDB tests (8). Both of these load cases are only performed on the near-side. On one hand, the Oblique Side Pole test consists in an onlique (75º) side impact of a vehicle against a rigid pole at a speed of 32 km/h. In this loadcase a WorldSID 50th Percentile Adult Male Dummy is placed in the driver position. On the other hand, the Side AE-MDB barrier consists in a test where the tested vehicle is impacted at 50 km/h by a Movable Deformable Barrier (AE-MDB Barrier). The test is performed with a WorldSID 50th Percentile Adult Mail Dummy in the Driver Position and a Q10 and a Q6 child dummies in the rear row seating in their respective child restraints. Additionally, from 2018 onwards, the far-side impact tests will also need to be performed (the first t20 years only for monitoring purposes). A frst draft of this protocol has already been released by Euro NCAP (9).

According to this first version of the document, the Far-Side Assessment Testing protocol will consist in two sled tests that will be performed with the Body in White (BiW) mounted on a sled with the centerline at 75º ± 3º towards the direcvtion of travel. The sled pulses to be used in the tests will be: the pulse for a representative AE-MDB-to-car test at 60km/h and the pulseof a 32 km/h 75º pole test. Both Pulses will be taken from the vehicle's non-strucc side B-Pillar Pulse. The only occupant to be included in these tests will be a WorldSID 50th percentile adult male dummy seated in the driver position. Figure 2 (found below) shows a simplified shematic of this test configuration.

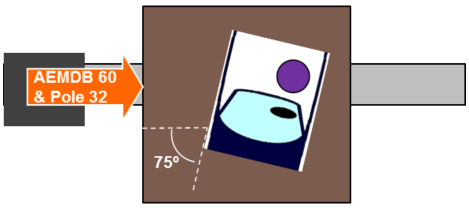

Fig. 2 Far-Side Sled Test Configuration.

The Far-Side Impact Assessment rating will be based on a combination of: the occupant Injury Criteria Results obtained from the WorldSID 50th Percentile Adult Male Dummy and the evaluation of whether the dummy exceedes the Head Excursion Lines that have been defined in the protocol. This paper focuses on the latter, the evaluation of the dummy head excursion in far.side assessment tests.

Figure 3 shows a graphic representation of the different head excursion lines that will be considered for the far-side assessment evaluation. In this protocol, the blue line corresponds to the vehicle centerline, the green line represents the occupant-to-occupant interaction line (centerline + distance corresponding to half of the shoulder width for a 95th percentile adult male dummy = 250mm), the yellow line indicates the far-side front seat centerline and the red line corresponds to the maximum door trim intrusion.

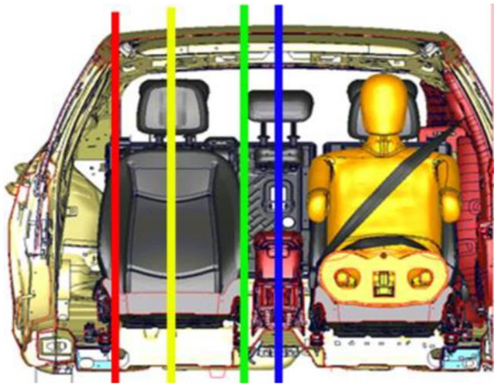

Fig. 3 Vehicle Markings for Far-Side Assessment Tests (9).

The evaluation of the occupant head excursion performance of the vehicle under the far-side impact testing load cases will be evaluated by assessing whether the occupant head crosses the previously indicated lines. To do this, three on-board cameras will be positioned in the vehicle. Each camera will be centered on the excursion lines to be evaluated (Red, Yellow and Green). The evaluation of the head excursion, then, will be made by film analysis of each of the camera views that are centered on the head excursion lines. An image showing the camera positions required for these tests may be found below:

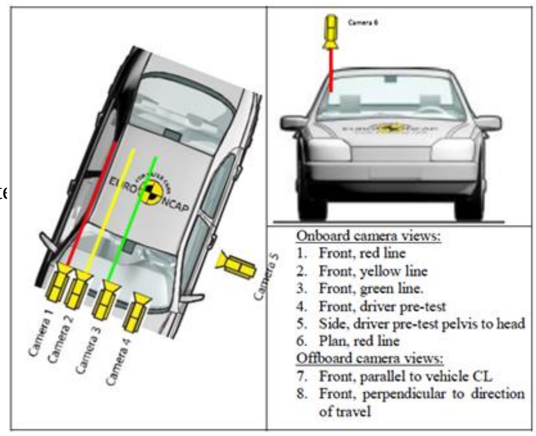

Fig. 4 Required camera positions for Far-Side Tests (9)

However, this evaluation method has its limitations. Although it is an excellent method for head excursion evaluation in official tests; during the vehicle development phases, vehicle manufacturers are likely to want to know which is the maximum dummy head excursion in a quantitative way, not only whether it exceeds the line or not. This can facilitate the control and progress of this assessment in different phases of the project. For this reason, IDIADA has developed an alternative methodology for far-side head excursion evaluation.

3. IDIADA TRACKING METHODOLOGY FOR EURO NCAP FAR SIDE EVALUATION

In this section the tracking methodology used to measure and evaluate the far side test in Applus IDIADA is explained. The results obtained through this methodology will help Applus IDIADA’s customers to determine and monitor the status of the vehicle development in terms of the new Far Side Euro NCAP protocol.

3.1. Tracking service in IDIADA

The main purpose of the IDIADA tracking service is to provide relevant information such as velocities, accelerations, displacements and deformations extracted from the images recorded in automotive testing by means of photogrammetry and center point detection algorithms.

Photogrammetry has been defined by the *American Society for Photogrammetry and Remote Sensing* (ASPRS) as the “art, science and technology” of obtaining useful information from the real world through “recording, measuring and interpreting photographic images”(10). Thus, by applying a combination of point detection algorithms on images acquired with calibrated imaging systems, IDIADA can provide precise information of the real 3D position in time of any visible point in the recorded images.

3.1.1. Camera-lens calibration

One of the key points when working in photogrammetry and computer vision is the photogrammetric calibration (11). This process is mandatory for any tracking measurement and it can be performed by taking images of a calibrated object whose 3D measures in the real world are known or via ‘self-calibration’; just moving twice an imaging system in a static scene and finding correspondences between the fixed internal parameters of the camera. Thus, in order to achieve a very robust and efficient calibration, IDIADA uses a calibration board, as the one showed in Figure 5, to calibrate the camera-lens systems involved in tracking analysis.

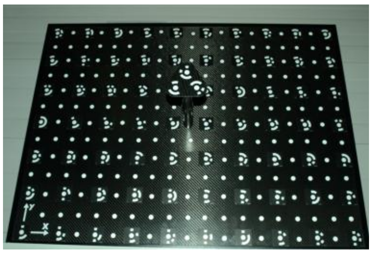

Fig.5 Rigid carbon fiber board used in IDIADA for photogrammetric calibration.

Every fiducial marker on the calibration board has been precisely measured in advance and its 3D coordinates in the real world are then well-known. For this, when taking a picture of the calibration board with an imaging system (i.e. camera equipped with a fixed lens) all the internal parameters of the system such as the focal length, the image sensor format and the principal point can be calculated (12).

Furthermore, given a set of pictures of the calibration board from different points of view, the geometry of the scene, the motion parameters and the optical carachteristics such as radial distortion of the imaging system acquiring that pictures can be described through the image projection of all the measured points by the bundle adjustment process, which is nowadays broadly used in computer vision research and calibration (13).

3.1.2. Tracking algorithms

The most common tracking algorithms used by Applus IDIADA and the automotive industry to determine the position of a real object are the so-called ‘Correlation’, ‘Quadrant’ and ‘MXT Tracker’ algorithms. They will be useful depending on the application and conditions of the test:

- **Correlation**: this algorithm searches for the area that correlates best with a previously-set pattern inside a specific region of each image in a stack and can be used for most of the industry applications.

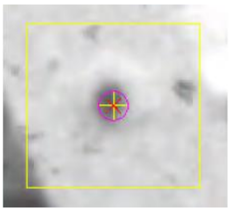

Fig.6 Correlation algorithm

- **Quadrant**: in this case the algorithm defines the central point by finding the symmetry centre of the Quadrant marker. This marker has been commonly used in the automobile market since it is rotationally invariant and can be also recognized by image color segmentation.

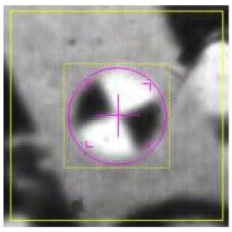

Fig.7 Quadrant algorithm

- **MXT**: by recognizing the white dots inside the MXT marker, this algorithm finds the centroid that is used to calculate the position of a real object given an image. The high contrast between the white dots and the black background of the MXT marker gives to the algorithm the best robustness and precision when computing the position of the centroid. That's why the MXT will be the algorithm used to evaluate the Far Side test.

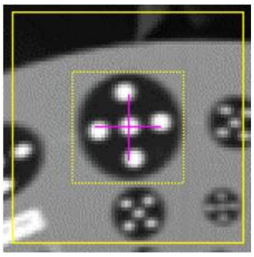

Fig.8 MXT algorithm

3.1.3. Three dimensional tracking and 6DOF

Based on the algorithms explained before the tracking service can be offered from two different approaches: the three dimensional (3D) tracking and the six degrees of freedom (6DOF) tracking.

The first one requires two or more calibrated imaging systems and some fixed markers present in the films acquired with the cameras to calculate the 3D position of those targets in the real scene. All these cameras involved should observe the markers from different points of view and share part of the field of view to be able to follow them and analyze their trajectories, giving as a result the desired 3D information in time of each point.

On the other hand, given a rigid body with at least four previously measured markers, whose 3D real positions are well-known, it is possible to calculate their 6 degrees of freedom with a single camera along the full movie. The 6DOF are the X, Y and Z position coordinates and the yaw, pitch and roll attitude angles (Figure 9), which can be computed for any point of the tracked rigid body even the if those studied point are not seen for the camera due to occlusion as long as it is possible to see the four measured markers.

Then, using the 6DOF tracking approach, the trajectory of several points on the dummy head can determine the position and rotation of the entire head. The possibility of knowing where the rigid body is located inside the car during the test can led to multiple calculations that could be taken into account in the new far side protocol, such as the minimum distance between two different objects, the angular and linear velocity or the acceleration of the dummy head, etc.

The uncertainty calculation for the 3D and 6DOF methods is complex and variable depending on the test performance since several differences on the initial measurements can affect the resulting uncentainty. Nevertheless, further investigation on the 6DOF uncertainty can provide information to reduce those circumstances, establish a robust protocol and obtain the best positional tracking possible.

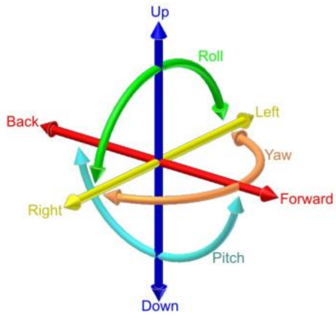

Fig.9 Representation of the six degrees of freedom that can be measured with the tracking methodology.

3.2. Far Side tracking procedure and assessment

Taking advantage of the tracking measurement IDIADA has been working on a specific methodology that can evaluate the position of the dummy head at any time of the far side test.

3.2.1. Test preparation for Tracking

Several factors of the real scene can affect the final results in the tracking calculation. For this, it is important to set-up and configure the test before it is performed in order to have the minimum error for the tracking post analysis.

Thus, in IDIADA the Far Side test will involve a single high-speed camera for the evaluation of the dummy head excursion with the 6DOF tracking methodology. This previously calibrated high-speed camera should be adjusted in order to have a good exposure and contrast of the markers in the scene. Furthermore, the camera configuration must ensure no motion blur of the targets in the film since it has severe affectations on the marker centroid computation. On the other hand, the location and illumination of the markers will also be relevant for the far side evaluation. The lightning systems should be setted-up to guarantee that the scene will be bright enough during the whole test and the target position on the dummy head should be as shown in Figure 10.

Fig.10 MXT marker position on the dummy head.

It is essential to see at least four markers during the full movie of the test to track the complete performance of the head and triangulate the 3D location of the dummy head points into the real scene and validate the far side test results.

The vehicle and dummy head reference points should be previously measured with the highest precision. To do so, the *coordinate measurement machine* (CMM) is one of the best tools performing these task [R6]. The coordinate system can be changed with the CMM at any time, providing a control of the measured head reference points respect to the vehicle ones.

Apart from the reference points in the vehicle structure, the entire dummy head will have to be scanned prior to the test performance (Figure 11). With this, it is possible to obtain a virtual representation of every 3D point on the surface of the dummy head. Then, the position in time of the head model can be virtually representated with the trajectories calculated applying the current tracking method.

Fig.11 In the left picture a handheld scanner to measure the dummy head surface is presented. In the right image a generated virtual mesh from the data obtained with the scanner can be seen. Analysis of the contrast and correlation of details in the captured picture by the scanner, calculates points in the 3D environment. Reference points reposition the 3D model to the coordinate system of the vehicle.

3.2.2. Evaluation of the Far Side test results

To validate the tracking method applied to the new far side protocol, a series of sled test have been carried out following the explained procedure. These tests provided relevant information to understand the performance of the tracking and have determined how the different configurations can affect the uncertainty of the tracking method.

The initial validation has shown that the uncertainty results calculated in standard conditions could increase up to 5mm but, applying the more than 20 years of testing knowledge, IDIADA has been able to reduce the margin of error to less than 1,5mm.

This has been possible by looking for the best illumination conditions and high-speed camer locations to guarantee the best images of the markers during the test so that the required information can be precisely measured.

In the new far side protocol Euro NCAP evaluates the head excursion blue, green yellow and red marks displayed on the videos. Thus, the assessment protocol only considers the maximum displacement of the dummy head for the Y axis relative to the vehicle’s coordinate system , defined in Figure 12, for the evaluation.

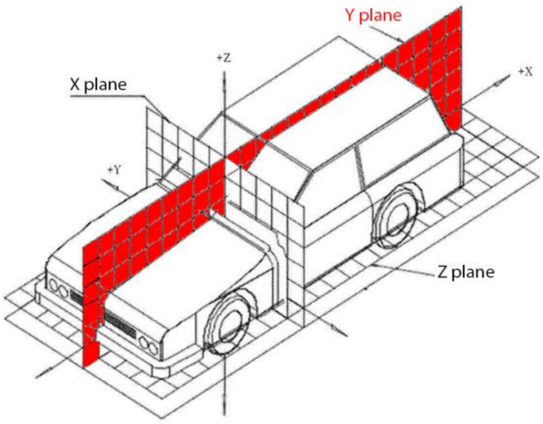

Fig.12 Representation of the Y plane, which is evaluated in the far side protocol. With the 6DOF tracking method it is also possible to compare the dummy head movements with X and Z planes of the vehicle coordinate system.

The plot generated with data from the 6DOF tracking method of a far side test is presented in Figure 13. The values have been altered in this case in order to guarantee the confindenciality agreements from IDIADA.

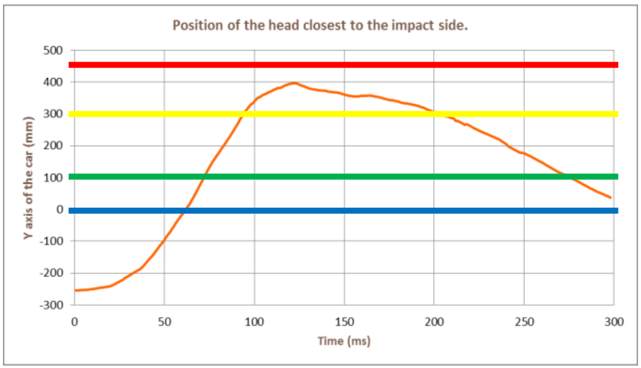

Fig.13 Plot showing the displacement in the Y axis of the dummy head respect to the coordinate system of the vehicle in a far side test. Presented data has been modified for public purpose.

Considering the blue line as the centerline of the vehicle, and thus the value 0 in the Y axis coordinate system, the dummy head in this test is moving from an initial distance of 250mm to 397mm from the center of the vehicle, crossing the blue, the green and the yellow excursion lines. This plot proofs that the 6DOF tracking methodology fulfills the Euro NCAP far side test protocol assessment. Furthermore, the relevant data for evaluating the performance of the test is shown in table 2:

Table 2 Head excursion values from a far side test

	Y axis position	Crossing time
Blue Line	**0 mm**	**63 ms**
Green Line	**100 mm**	**71 ms**
Yellow Line	**300 mm**	**94 ms**
Red Line	**450 mm**	**NO**
Maximum	**397 mm**	**122 ms**

However, using the 6DOF tracking methodology it is possible to evaluate not just if the head crosses the excursion lines or not, but also the exact 3D position of the dummy head respect to the vehicle. The generated data is taken into account to determine if the saftey systems of the vehicle are improving the results with and without the passenger and also if the far side door trim intrusion is working as intended

For example, the tracking methodology could provide information about if the dummy is close to other objects such as the steering wheel or the dashboard during the test. Thus, it is possible to know the exact position respect to other parts of the vehicle to be able to evaluate all the possible risks when performing the test.

Other elements such as the dummy head movement with respect to the body could be analyzed to observe the behavior of the neck during the test.

Nevertheless, the deployment of airbag restraint systems for the far side protection could imply a lack of visualization of the dummy head maximum displacement during the test, complicating the protocol assessment. Despite of that, the 6DOF tracking methodology is able to determinate if the dummy head has crossed the excursion lines without seing the entire dummy head in the movie.

The strategic target position methodology ables the tracking algorithm to compute trajectories and calculate the position of the dummy head at every moment as long as at least four markers are seen by the high-speed camera. Since the dummy head has been previously scanned and measured, with this technique it is possible to analyze the interaction of the dummy head with any element in the vehicle without seing it. In Figure 14 a virtual representation of the minimum distance of the dummy head with the steering wheel is presented.

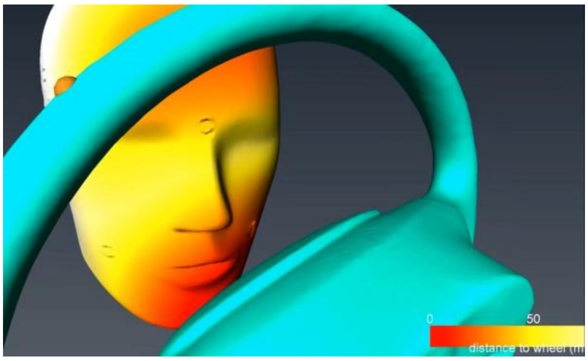

Fig.14 Virtual model showing the minimum distance of the dummy head respect to the steering wheel.

This virtual representation has been generated from real data obtained in a frontal crash test. In the moment of minimum distance between the dummy head and the steering wheel the frontal airbag was completely deployed and so the entire head was covered by the bag. Thus, the 6DOF tracking method was still able to provide relevant and precise information about the dummy head and steering wheel interaction.

This methodology can be very useful to analyze the far side test. The analysis of the dummy behavior during the test and the comparison between other sled tests can provide necessary data to study the performance of the restraint systems of the vehicles in the development phase.

4. CONCLUSIONS

Recent traffic accident data from different countries in Europe have impulsed the development of a new far side test protocol by Euro NCAP, which will become an official test by the year 2020 and which tends to reduce the likelihood of sustaining moderate injuries of the vehicle occupants involved in far side lateral crashes.

This new protocol will evaluate if the driver dummy head excursion crosses the door trim maximum intrusion, the passenger seat centerline, the occupant to occupant interaction line and/or the vehicle centerline in a sled test. In order to assess the test, the protocol suggests to set-up several high-speed camera centered on the mentioned excursion lines to visually check wether the dummy head crosses the lines or not during the test.

However, the tracking methodology presented in this article uses a single camera and a series of MXT markers to determine the displacement and rotation of the dummy head during the full recorded movie of the test. With this procedure, IDIADA is able to provide information about not only if the dummy head crosses a specific excursion line to assess the Euro NCAP far side protocol but also how much the development of the driver restrain systems improve or not the results of the test.

This methodology can be specially interesting during the current test monitoring phase for both Euro NCAP and automobile OEM's since the precise information obtained with the 6DOF tracking methodology can help to adjust the evaluation ratings for the new Euro NCAP far side test protocol and also let the manufacturers know if they're developing the restraint safety systems in terms of reducing the far side crash injuries.

REFERENCES

(1) Insurance Institute for Highway Safety (IIHS) – General statistics – Fatality facts – Passenger vehicle occupants – 2016: http://www.iihs.org/iihs/topics/t/general-statistics/fatalityfacts/passenger-vehicles#Crash-types

(2) Euro NCAP. "The Ratings Explained. Adult occupant Protection. Side Mobile Barrier": https://www.euroncap.com/en/vehicle-safety/the-ratings-explained/adult-occupant-protection/side-mobile-barrier/

(3) Euro NCAP Side Impact Working Group. ACEA – Far Side Accident Analysis for Euro NCAP –V6. Reference Number SID-1604-02

(4) Wikipedia – Abbreviated Injury Scale - Severity: https://en.wikipedia.org/wiki/Abbreviated_Injury_Scale#Severity

(5) GIDAS: German In-Depth Accident Study http://www.gidas.org/

(6) Euro NCAP. "Euro NCAP 2025 Roadmap – In pursuit of Vision Zero – 12th September 2017 – Page 17": https://cdn.euroncap.com/media/30700/euroncap-roadmap-2025-v4.pdf

(7) Euro NCAP "Oblique Pole Side Impact Test Protocol, v7.0.3, November 2017 ": https://cdn.euroncap.com/media/32289/euro-ncap-pole-protocol-oblique-impact-v703.pdf

(8) Euro NCAP "Side Impact Mobile Deformable Barrier Test Protocol, v7.1.3, November 2017 ": https://cdn.euroncap.com/media/32291/euro-ncap-side-protocol-ae-mdb-v713.pdf

(9) Euro NCAP "Far Side Test $ Assessment protocol, v1.0, November 2017" : https://cdn.euroncap.com/media/32284/euro-ncap-far-side-test-and-assessment-protocol-v10.pdf

(10) The American Society for Photogrammetry and Remote Sensing (ASPRS) – "What is ASPRS?": https://www.asprs.org/organization/what-is-asprs.html

(11) Z.Zhang (2000) "A Flexible New Technique for Camera Calibration" - IEEE Transactions on Pattern Analysis and Machine Intelligence, Vol 22

(12) Directions for the calibration of cameras with an AICON target panel: https://www.falcon.de/falcon/pdf/en/aicon/calibration_of_cameras.pdf

(13) B. Triggs; P. McLauchlan; R. Hartley; A. Fitzgibbon (1999). "Bundle Adjustment — A Modern Synthesis". ICCV: Proceedings of the International Workshop on Vision Algorithms. Springer-Verlag. pp. 298–372

講演番号：118　文献番号：20185118

学術講演会予稿集正誤表

（Errata of Proceedings/Summarized Papers）

学術講演会セッション番号・セッション名 (SessionNo.-Session Name)	28 二輪車の運動・制御・安全（1）　−自動二輪車，自転車，PMV の未来に向けて−
講演タイトル（Title）	講演番号 118 自動二輪自立制御機構の研究
講演者名 (Speaker name) 所属名 (Affiliation)	辻井 栄一郎 ヤマハ発動機株式会社
誤 (Incorrect)	P2　24 行目 約 0. 5 度ていど
正 (Correct)	約 5 度ていど

講演番号：124　文献番号：20185124

学術講演会予稿集正誤表

(Errata of Proceedings/Summarized Papers)

学術講演会セッション番号・セッション名 (SessionNo.-Session Name)	29 二輪車の運動・制御・安全（2）ー自動二輪車，自転車，PMV の未来に向けてー
講演タイトル（Title）	内傾型パーソナルモビリティビークルの急操舵時内輪浮き特性
講演者名 (Speaker name) 所属名 (Affiliation)	原口　哲之理 （名古屋大学）
誤 (Incorrect)	Proceedings P2, Line15：研究報告 (4) P2, Formula (3)：f f ; Steering input frequency P4, Line7：式 (3) P4, Line13：式 (3) Summarized Papers Formula (1)：f f ; Steering input frequency
正 (Correct)	Proceedings P2, Line15：研究報告 (2) (3) (4) P2, Formula (3)：$f\varphi$ $f\varphi$; Roll resonance frequency P4, Line7：式 (4) P4, Line13：式 (4) Summarized Papers Formula (1)：$f\varphi$ $f\varphi$; Roll resonance frequency

講演番号：370　文献番号：20185370

学術講演会予稿集正誤表

(Errata of Proceedings/Summarized Papers)

学術講演会セッション番号・セッション名 (SessionNo.-Session Name)	82 自動車の運動と制御 Ⅳ ～乗り心地と自動運転技術～
講演タイトル （Title）	専用センサレスセミアクティブサスペンション向け 車両状態推定アルゴリズムの開発
講演者名 (Speaker name) 所属名 (Affiliation)	奈須 真吾 日立製作所
誤 (Incorrect)	$\begin{cases} F_{sfl} = k_{sf} z_{21fl} + c_{sfl} \dot{z}_{21fl} + k_{stf}(z_{21fl} - z_{21fr}) \\ F_{sfr} = k_{sf} z_{21fr} + c_{sfr} \dot{z}_{21fr} - k_{stf}(z_{21fl} - z_{21fr}) \\ F_{srl} = k_{sr} z_{21rl} + c_{srl} \dot{z}_{21rl} + k_{str}(z_{21rl} - z_{21rr}) \\ F_{srr} = k_{sr} z_{21rr} + c_{srr} \dot{z}_{21rr} - k_{str}(z_{21rl} - z_{21rr}) \end{cases} \quad \# \quad (1)$
正 (Correct)	$\begin{cases} F_{sfl} = k_{sf} z_{21fl} + \underline{c_{sf}} \dot{z}_{21fl} + k_{stf}(z_{21fl} - z_{21fr}) + \underline{F_{sdfl}} \\ F_{sfr} = k_{sf} z_{21fr} + \underline{c_{sf}} \dot{z}_{21fr} - k_{stf}(z_{21fl} - z_{21fr}) + \underline{F_{sdfr}} \\ F_{srl} = k_{sr} z_{21rl} + \underline{c_{sr}} \dot{z}_{21rl} + k_{str}(z_{21rl} - z_{21rr}) + \underline{F_{sdrl}} \\ F_{srr} = k_{sr} z_{21rr} + \underline{c_{sr}} \dot{z}_{21rr} - k_{str}(z_{21rl} - z_{21rr}) + \underline{F_{sdrr}} \end{cases} \quad \# (2)$

講演番号：415　文献番号：20185415

学術講演会予稿集正誤表

(Errata of Proceedings/Summarized Papers)

学術講演会セッション番号・セッション名 (SessionNo.-Session Name)	セッション番号：91 セッション名：潤滑油・潤滑技術およびトライボロジー (SessionNo.91 Lubricants, Lubrication Technology and Tribology)
講演タイトル （Title）	可視化エンジンを用いたピストン周りのオイル挙動計測 －フォトクロミズム用いた可視化手法による低温低速条件における検討－ (Measurement of Oil Transport Phenomena around Piston using Optical Engine -Investigation under Low Temperature and Low Speed Condition using Photochromic Visualization Technique-)
講演者名 (Speaker name) 所属名 (Affiliation)	倉辻風樹 (Kazaki Kuratsuji) 東海大学大学院 (Tokai University)
誤 (Incorrect)	Proceeding P.2 Fig.3 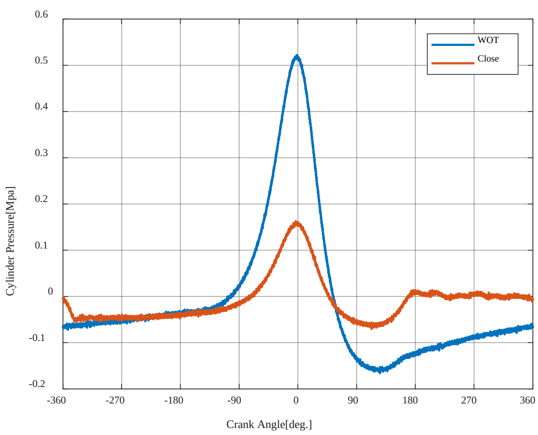
正 (Correct)	Proceeding P.2 Fig.3 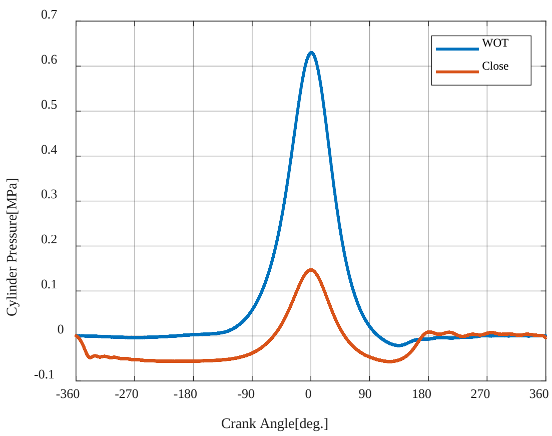

講演番号：440　文献番号：20185440

学術講演会予稿集正誤表

(Errata of Proceedings/Summarized Papers)

学術講演会セッション番号・セッション名 (SessionNo.-Session Name)	自動車技術会 2018 春季大会学術講演会 96・xEV 技術 I (SessionNo 96 -xEV Systems I)
講演タイトル （Title）	非接触充電における金属異物の発熱量の最大値に関する研究 (A Study on Maximum Heat Value of Foreign Metal Object at Wireless Charging)
講演者名 (Speaker name) 所属名 (Affiliation)	橋本俊哉 (Toshiya Hashimoto) トヨタ自動車株式会社 (TOYOTA MOTOR CORPORATION)
誤 (Incorrect)	・Fig. 16, 17, 20 凡例の Nickel と Carbon steel が逆 ・Fig. 18, 19 グラフ差し替え ・4. 2. 導出式に対する考察 直径が小さくなるにつれ温度上昇量は大きくなり．今回比較した材料では鉄コバルト合金が最大となる．しかし，ユースケースとしては円柱が空中に浮いていることはないため，接触による熱伝導も考慮する必要がある． ・5. まとめ 2) 棒形状の金属を磁界に対し平行に置いた場合，細くなるほど温度が高くなる．但し，温度上昇が最大となる太さの特定には，ユースケースにおける接触による熱伝導の考慮が必要である． 3) 棒形状の金属を磁界に対し垂直に置いた場合，温度が高くなる太さが材料で異なり極値を持つ．
正 (Correct)	次ページ参照

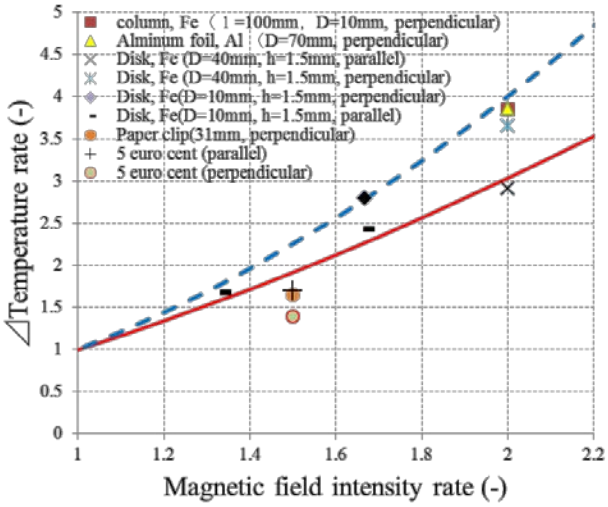

Fig.13 Relation Between △Temperature and Magnetic Field Intensity

Fig.14 は鉄の円柱（直径 10mm，長さ 100mm）を磁界に対し垂直に置いた場合と平行に置いた場合の温度上昇量の比を示したものである．本稿で導出した結果を実線で示しているが，実験値及び CAE にて算出した値とほぼ一致することがわかる．

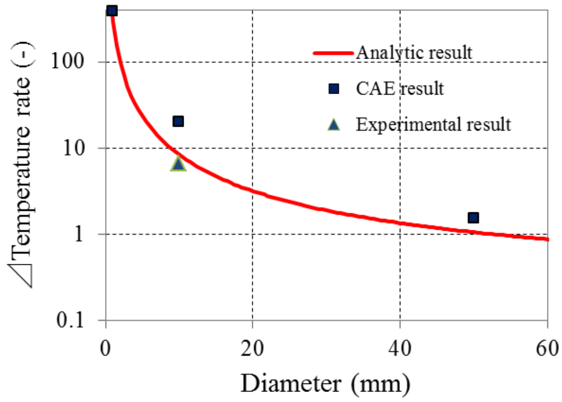

Fig.14 Relation Between △Temperature and Diameter

Fig.15 は鉄の円盤の温度上昇量について，実験結果及び CAE にて算出した値と比較したものである．発熱量から温度上昇量への変換は式(29)を用いた．ほぼ一致する結果となった．

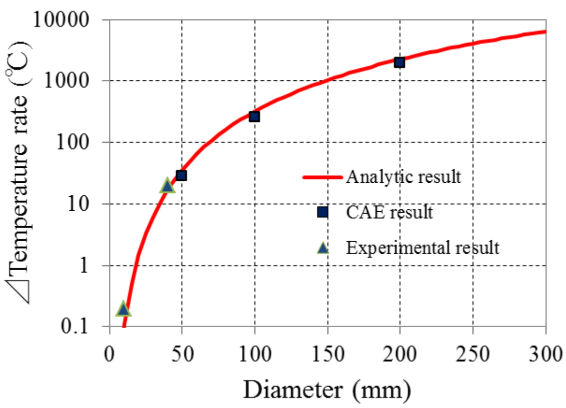

Fig.15 Comparison of Analytic Result and CAE Result

4.2. 導出式に対する考察

発熱量の式(20)(23)より透磁率及び導電率に対する円柱（直径 10mm，長さ，100mm）の発熱量の関係を Fig.16，17 に示した．磁界に対し垂直に置いた場合，もっとも発熱量が大きくなる極値が存在することがわかる．一方，平行に置いた場合，導電率が小さく，透磁率が大きいほど発熱量が大きくなることがわかる．

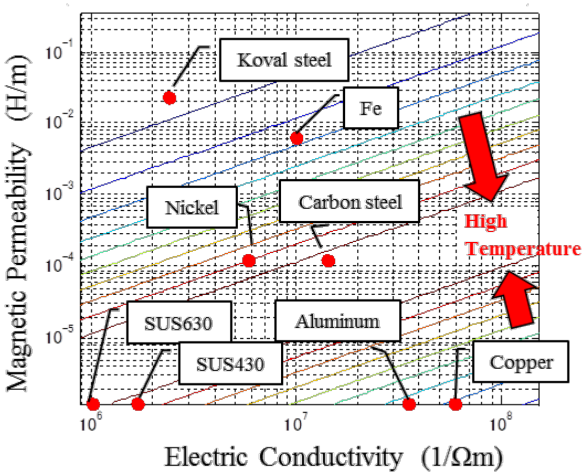

Fig.16 Relation Between Heat Value and Magnetic Permeability and Electric Conductivity (Perpendicular)

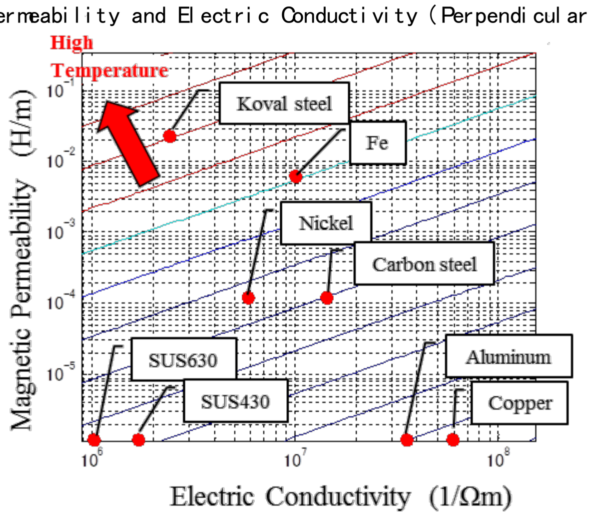

Fig.17 Relation Between Heat Value and Magnetic Permeability and Electric Conductivity (Parallel)

Fig.18 は鉄，鉄コバルト合金，炭素鋼，SUS430，銅の円柱を磁界に対し垂直に置いた場合の直径に対する温度上昇量を示したものである．直径が小さい場合，導電率より透磁率の影響が強くなり銅の温度上昇が最大となる．直径が大きくなるにつれ，導電率の影響が大きくなり，鉄や炭素鋼の温度上昇が大きくなる．Fig.19 は円柱を磁界に対し平行に置いた場合の直径に対する温度上昇量を示したものである．温度上昇量は直径にかかわらないことがわかる．

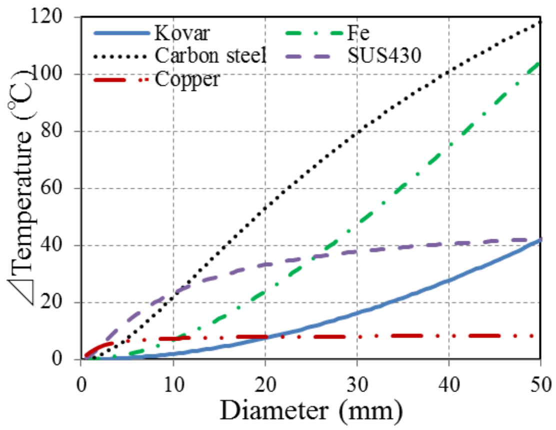

Fig.18 Relation Between ⊿Temperature and Diameter
(Analytic Result, Perpendicular)

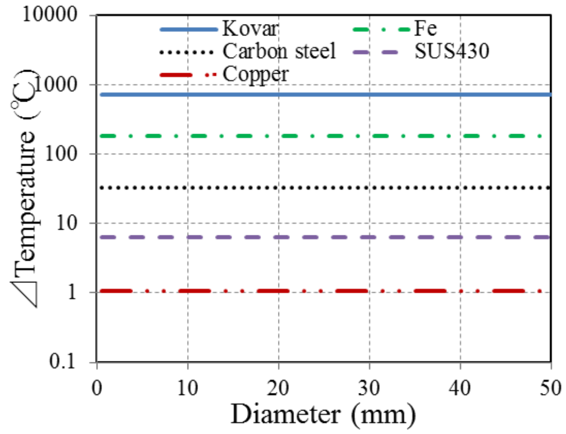

Fig.19 Relation Between ⊿Temperature and Diameter
(Analytic Result, Parallel)

発熱量の式(28)より透磁率と導電率に対する円盤（直径100mm）の発熱量の関係を Fig.20 に示した．透磁率及び導電率が大きくなるほど発熱量も大きくなることがわかる． 今回比較した材料では鉄が最大となる．

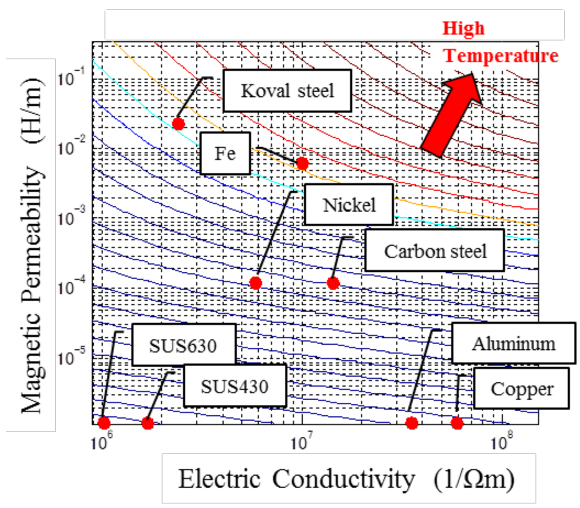

Fig.20 Relation Between Heat Value and Magnetic Permeability and Electric Conductivity (Disk)

Fig.21 は鉄，鉄コバルト合金，炭素鋼，SUS430，銅の円盤の直径に対する温度上昇量を示したものである．直径が大きくなるにつれ，温度上昇量が大きくなることがわかる．

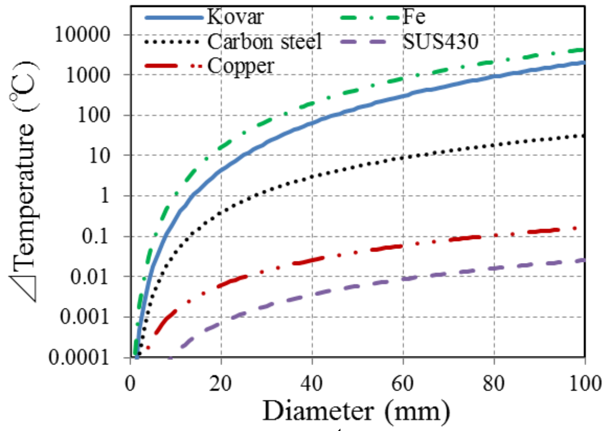

Fig.21 Relation Between ⊿Temperature and Diameter
(Analytic Result, Disk)

5. まとめ

本稿では非接触充電コイル間に金属物を置いた場合の温度について，Maxwell 方程式を摂動的に解くことで，解析解を得ることができた．また，それは温度上昇量に対する形状，配置について実験結果とほぼ一致した．解析解を考察することで，発熱量が大きくなる材料や形状の特性を理解することができた．

1) 温度は形状や配置方向によらず磁界の強さの 1.6～2 乗で上昇する．
2) 棒形状の金属を磁界に対し平行に置いた場合，直径に関係せず温度上昇量は決まり，透磁率／導電率の比が大きい材料ほど高くなる．
3) 棒形状の金属を磁界に対し垂直に置いた場合，温度が高くなる材料は透磁率／導電率の比で決まり，その値は太さ及び周波数の関数で決定することができる．
4) 棒形状の金属は，透磁率／導電率の比が最大となるものを磁界に対し平行に置いた場合，温度上昇が最大となる．
5) 円盤形状の金属を磁界に対し垂直に置いた場合，直径が大きくなるほど温度が高くなる．また，透磁率及び導電率が大きいほど温度が高くなる．

参 考 文 献

(1) 駒崎，他：電気自動車用非接触給電装置のギャップ中の異物検知法，電気学会産業応用部門大会 No.4-10 (2012)
(2) 鳩野：ワイヤレス給電システムにおける FOD 理論的解析モデルの提案，電子情報通信学会技術研究報告 06-06 (2014)